Sensory Experience Restructures Thalamocortical Axons during Adulthood

Marcel Oberlaender[1,3], **Alejandro Ramirez**[2,3], and **Randy M. Bruno**[2,*]

[1]Digital Neuroanatomy, Max Planck Florida Institute, Jupiter, FL 33458, USA

[2]Department of Neuroscience and the Kavli Institute for Brain Science, Columbia University, New York, NY 11032, USA

SUMMARY

The brain's capacity to rewire is thought to diminish with age. It is widely believed that development stabilizes the synapses from thalamus to cortex and that adult experience alters only synaptic connections between cortical neurons. Here we show that thalamocortical (TC) inputs themselves undergo massive plasticity in adults. We combined whole-cell recording from individual thalamocortical neurons in adult rats with a recently developed automatic tracing technique to reconstruct individual axonal trees. Whisker trimming substantially reduced thalamocortical axon length in barrel cortex but not the density of TC synapses along a fiber. Thus, sensory experience alters the total number of TC synapses. After trimming, sensory stimulation evoked more tightly time-locked responses among thalamorecipient layer 4 cortical neurons. These findings indicate that thalamocortical input itself remains plastic in adulthood, raising the possibility that the axons of other subcortical structures might also remain in flux throughout life.

INTRODUCTION

Numerous studies have concluded that the thalamocortical (TC) projection, along which sensory information flows into the cerebral cortex, is fixed by the end of development. During a critical period in early postnatal life, monocular vision loss can trigger robust anatomical plasticity of TC axons in the mouse and cat visual systems (Antonini et al., 1999; Antonini and Stryker, 1993). Such anatomical changes are thought to be driven, at least in part, by the strengthening and weakening of existing TC synapses, which in slices of somatosensory cortex cannot be induced beyond the first few postnatal weeks, probably due to the known developmental downregulation of NMDA receptors (Feldman et al., 1999). In both the visual and somatosensory systems, sensory experience during adulthood has little or no effect on the receptive fields of neurons in cortical layer 4 (L4) but has robust effects on other layers (reviewed in Feldman and Brecht, 2005; Fox, 2002; Karmarkar and Dan, 2006). From such physiological studies, it has been inferred that adult plasticity, learning, and memory is mediated by functional and/or anatomical changes among corticocortical connections (De Paola et al., 2006; Feldman and Brecht, 2005; Fox, 2002; Karmarkar and Dan, 2006).

A purely cortical locus for adult plasticity has, however, recently become controversial. Brief periods of monocular deprivation can alter the size of pharmacologically isolated TC-evoked field potentials in adult mouse visual cortex (Khibnik et al., 2010). Whisker trimming for as few as 3 days similarly reduces the overall density of TC synapses in adult rat barrel cortex (Wimmer et al., 2010). These recent findings prompted us to investigate the effect of sensory experience during adulthood anatomically on individual TC axons and functionally on the magnitude and synchrony of cortical activity.

We manipulated sensory experience in adult (3-month-old) rats using a painless, nondestructive approach. Trimming the large facial whiskers alters sensory experience without engaging potential trophic mechanisms that might be triggered by plucking whiskers or lesioning whisker follicles. Individual thalamocortical neurons were filled in vivo by whole-cell recording and reconstructed in three dimensions via a recently developed semiautomatic method. We discovered that TC axonal arbors remain plastic in adulthood, with whisker trimming causing axons originating from the deprived representation to lose on average a quarter of their length across layers. Within L4, axonal branch reduction was higher and topographically specific. Dual cell-attached recordings in vivo revealed that sensory stimuli evoked greater levels of synchrony among L4 neurons but the same number of action potentials from individual cells. Our findings demonstrate that adult plasticity is not limited to corticocortical connections and potentially explain why previous functional studies of L4 could not infer such massive anatomical changes.

RESULTS

Conventional bulk tracers label the axons of many neurons, whose overlap confounds their reconstruction and quantification. Whole-cell recording, while challenging to obtain from a cell ~5 mm deep within the brain, robustly labels a single axon when successful, facilitating unambiguous tracing (Bruno et al., 2009). We therefore patched a single thalamocortical neuron in the ventral posterior medial thalamic nucleus in each of 28 adult rats. All the large facial whiskers except two had been trimmed daily (deprived group) or sham trimmed (control group) for the preceding 13–27 days. Cages were not left empty but instead were enriched with cardboard boxes and tubes to encourage whisker-based exploration of the environment, which has been suggested to enhance thalamocortical plasticity (Wimmer et al., 2010). In deprived rats, we filled neurons belonging to the trimmed whisker representation. Axons were three-dimensionally reconstructed with submicron resolution (Figures 1A and 1B; see Figure S1 available online) using a recent semiautomatic tracing system, which rivals human experts in both accuracy and completeness (Oberlaender et al., 2007, 2009, 2011). The combination of these filling and reconstruction approaches recovered total lengths of normal TC axons far greater than previously observed. Control axons ranged from 32.5 to 72.5 mm, with even the smallest TC arbor longer than those previously reported for rat barrel cortex or kitten visual cortex (Antonini and Stryker, 1993; Arnold et al., 2001).

Axons in control and deprived animals targeted barrels with similar spatial distributions, with no obvious spatial bias in our samples (Figure 1C). Average total length of individual axonal arbors within barrel cortex was 54.1 ± 3.7 mm for control animals (Figure 1D, black circles; mean $\pm$ SEM, n = 12). Simply trimming the whiskers significantly decreased the average length of axons corresponding to deprived whiskers by 25%, down to an average of 40.6 ± 4.7 mm (gray circles; n = 11, p = 0.017). Trimming similarly decreased the number of branch points by 32% (Figure 1E; control 232 ± 27 versus deprived 158 ± 17; p = 0.016). Due to the extreme depth of the thalamus, its complicated three-dimensional geometry, and the small size of individual thalamic "barreloids," we recovered only two axons corresponding to spared whiskers. Given that their lengths (46.5 and 37.7 mm) are in the

ranges of both control and deprived distributions, no inferences can be made regarding this small spared sample. Nevertheless, our results clearly demonstrate that innocuous sensory experience can substantially alter the structure of inputs to cortex in adulthood.

Barrel size is well known to depend on location within the barrel subfield. There was, however, no significant relationship of the length of thalamocortical axon to the size of the innervated barrel, regardless of whether control and deprived groups were analyzed separately or pooled (Figure 2A; all p values > 0.5). This surprising result suggests that the size of a barrel reflects the number of neurons in the corresponding thalamic barreloid, rather than the lengths of individual innervating axons. Consistent with this finding, the trimming-induced decrease in innervation is still significant even after normalizing the length of each axon by the area of its respective barrel (Figure 2B). Indeed, trimming appeared to impact axonal length relatively consistently across whisker arcs and rows (Figure 2C).

Other morphological features remained unaffected. Trimming produced no concomitant change in the area or height of the barrels innervated by these axons (Figures 2D–2F; p values > 0.1) consistent with previous studies (Fox, 1992). The areas innervated (field spans; Figures 2G and 2H) by both the superficial L3-L4 collaterals (Figure 2I) and the deeper L5/6 collaterals (Figure 2J; p values > 0.1) were stable. The distances between boutons along axons, putative synapses, were similarly unaffected by trimming (Figures 2K and 2L; p > 0.1). The experience-induced decrease in TC axonal length therefore appears to reflect an absolute reduction in afferent synapses, perhaps via pruning of specific branches.

Individual axons span multiple functionally distinct zones, such as different cortical layers (Figure 3A) and somatotopic columns (Figure 3C). We therefore considered how the effects of experience on synaptic connectivity might depend on cortical location. As in the visual and possibly auditory systems (Ferster and LeVay, 1978; Smith et al., 2012), TC axons were mainly "bistratified," with two distinct sets of collaterals at depths of 600–1,000 and 1,300–1,500 μm from the pia, corresponding to L4 and L5B-L6A, respectively (Figure 3B; Figure S1). Sensory deprivation impacted the total length of axon most noticeably at these depths, with both decreases being statistically significant (p values = 0.024).

We additionally subdivided each axon according to the locations of its branches relative to the column defined by the L4 barrel it targeted (Figures 3A and 3C). On average, a control TC axon had 57% of its branches in its targeted barrel column, 19% across multiple adjacent barrel columns, and 24% in the septal space between barrel columns. Inside the column (red), trimming significantly decreased total axonal length and branching (Figures 3D and 3E; from 30.8 ± 2.7 to 20.5 ± 3.3 mm, p = 0.012; from 161 ± 20 to 92 ± 16 branch points, p = 0.007). The absolute total length change inside the column derived mainly from a 37% reduction of axon in L4 (Figure 3D; from 19.8 ± 6.8 to 12.5 ± 7.7 mm; p = 0.015). Branches in L2/3 and L5/6 exhibited proportionally similar reductions (35% and 23%, respectively), although these reductions accounted for less of the absolute change within the column (from 3.2 ± 2.6 to 2.1 ± 2.0 mm for L2/3, from 7.7 ± 2.6 to 5.9 ± 3.2 mm for L5/6) and were either statistically insignificant or trend level (Figure 3D; p = 0.14 for L2/3, p = 0.055 for L5/6).

In contrast, branches lying beyond the column (Figures 3A and 3C; black and gray) displayed little or no change. In particular, axons lying in L4 outside the column are almost identical in length and branching between control and deprived groups (<1% difference; Figures 3F and 3G; p values > 0.1). Length reductions were again only trend level within L5/6 (26%; p = 0.08) and not significant in L2/3 (24%; p = 0.22). Thus, experience-induced restructuring of TC axons appears highly topographic within L4. If L2/3 and L5/6 are also indeed plastic, restructuring appears more distributed, not being restricted to the column.

These results indicate that, rather than being cell autonomous, plasticity of TC axonal branches depends on how they interact with specific cortical subnetworks.

Such substantial localized changes in thalamocortical connectivity would be expected to alter the functional properties of L4 neurons. Single-unit studies of both juvenile rat barrel cortex and cat visual cortex, however, have uncovered functional plasticity in L2/3 but not in L4 (Glazewski and Fox, 1996; Jacob et al., 2012; Trachtenberg et al., 2000). The resistance of L4 to manipulations of the periphery is widely believed to result from developmental downregulation of long-term potentiation and depression at the TC synapse, as observed in vitro (Feldman et al., 1999). Some in vivo studies have, however, reported short-latency (<10 ms) changes in L4 responses and have suggested that TC plasticity might still exist beyond adolescence (Wallace and Fox, 1999). We revisited this issue by performing simultaneous cell-attached recordings from two L4 neurons in the same barrel (Figure 4A, left).

Population peristimulus time histograms of L4 responses to sensory stimulation appeared similar for control and deprived groups (Figure 4A, middle), and their temporal profiles were also similar (Figure S2A). The deprived group had a slightly increased response (Figure 4A, right) as in previous studies (Glazewski and Fox, 1996), but this 14% increase in average evoked activity was not statistically significant (p = 0.36, 36 control and 43 deprived cells). Similarly, deprivation did not significantly affect spontaneous firing rates.

We and others have suggested, however, that sensory information may be more robustly propagated by near-synchronous discharges of presynaptic pools of neurons rather than by uncoordinated increases in firing rates (Bruno, 2011; Bruno and Sakmann, 2006). To assess synchrony, we initially plotted cross-correlation histograms for simultaneously recorded pairs of L4 neurons (Figure 4B; Figures S2B and S2C). Firing-rate-normalized cross-correlation histograms (Eggermont and Smith, 1996) for each group suggest that neurons in deprived animals are more likely to discharge action potentials within ~10 ms of one another (Figure 4C; Figure S2D). However, statistical comparison of time-based "cross-correlograms" is notoriously problematic.

A more rigorous way to quantify and statistically test correlated activity is to compute coherence, which re-represents spike trains in the frequency domain, where any two frequencies are statistically independent (Jarvis and Mitra, 2001). By definition, coherence ranges from 0.0 (no correlation) to 1.0 (identical trains of action potentials) and is intrinsically normalized by the firing rates of the two cells. The average coherence of the responses of simultaneously recorded neurons was increased by whisker trimming for all frequency components of the neural activity (Figure 4D). We calculated a single coherence value for each pair by averaging its coherence function over 4–20 Hz (23 control and 26 deprived pairs). On average, trimming significantly raised coherence (Figure 4D, inset; K-S test, p = 0.04), with the mean increasing from 0.126 to 0.250. Both groups contained a number of pairs with little or no coherence (coherence < 0.2), perhaps suggesting that correlation changes may be limited to only certain combinations of cell types. These time-domain (cross-correlation) and frequency-domain (coherence) analyses together indicate that sensory experience alters the synchrony of neuronal groups more than it detectably alters the absolute firing rates of individual cells.

All other things being equal, the reduced TC synaptic connectivity we found should decrease rather than increase L4 synchrony. Enhanced L4 synchrony suggests that experience alters an additional element of the circuit. One possibility is that the pruning of TC-L4 synapses triggers homeostatic rescaling of the strength of synapses—afferent and/or intracortical—onto an excitatory L4 neuron to maintain its normal firing rate. To check this,

we removed the stimulus-induced correlation to reveal millisecond-scale neural interactions. Near-synchronous events in a "raw" cross-correlogram (Figure 4B, bottom; Figure 4E, top) result from a pair of cells receiving shared common input(s) and/or being embedded in independent circuits whose activity is transiently modulated by the same stimulus. The stimulus-induced correlation can be estimated by shifting one of the spike trains by a stimulus trial and calculating a "shift corrector" (Figure 4E, middle). The difference of the raw correlogram and corrector is an estimate of shared input, synapses that derive from the same divergent axons. The millisecond-scale locking of such synapses produces a sharp peak in the correlogram (Figure 4E, arrow), which represents some unknown number of diverging fibers that contact both cells.

Significant shared inputs occurred in 13 out of 23 (57%) control pairs and 12 out of 26 (46%) trimmed pairs. For each of these significant pairs, we measured the strengths of shared inputs (Figure 4F). Trimming significantly increased the strengths of shared inputs (t test, p = 0.017). Enhancement of shared inputs is also visible in normalized population cross-correlograms, in which the relative sizes of the fast millisecond-scale component and slower stimulus-induced component differ between groups (Figure S2D). These results suggest that homeostatic strengthening of corticocortical synapses and/or unpruned thalamocortical synapses may parallel or follow TC synapse loss, thereby enhancing correlated activity in L4. Because the synchrony of a neuronal population can impact the response magnitude of its downstream targets (Bruno, 2011), experience-induced changes in L4 synchrony may constitute a previously unconsidered contributor to functional plasticity in layer 2/3 (Feldman and Brecht, 2005; Fox, 2002; Karmarkar and Dan, 2006).

DISCUSSION

Changes in corticocortical connectivity have long been thought to mediate adult plasticity. Our study reveals that thalamocortical axons also remain plastic in adulthood. Simply trimming whiskers, a nondestructive alteration in sensory experience, brought about a 25% decrease in total thalamocortical arborization. Furthermore, innervation of L4 was decreased by 37% in the targeted column with virtually no change of branches lying in L4 beyond the column borders. These findings, taken together with our previous bulk tracing results (Wimmer et al., 2010), indicate that such experience-dependent rewiring of the thalamocortical projection may occur in as little as 3 days. Rapid receptive field changes in any TC-innervated layer, as recently observed for L5 (Jacob et al., 2012), may partially derive from rapid rewiring of TC anatomy.

Given that interbouton distances along axons were unperturbed by trimming, our results indicate a striking reduction in the number of thalamocortical synapses. This reduction was highly unexpected because the sensory responses of single units in L4 are largely regarded as stable, whereas other layers seem robustly plastic (Feldman and Brecht, 2005; Fox, 2002; Karmarkar and Dan, 2006). We too observed that L4 response magnitudes are relatively stable. Our results demonstrate that single-unit recordings from a neuronal population do not necessarily allow the inference of anatomical changes among its inputs.

One possible explanation is that feedforward inhibition in the thalamocortical circuit maintains L4 responsiveness in the face of TC pruning. Trimming would simultaneously decrease both feedforward excitation and inhibition, possibly leaving L4 response magnitudes unchanged. In this scenario, other functional aspects of cortical activity, beyond the magnitude of sensory-evoked responses, might be plastic. Sensory information may be robustly encoded by near-synchronous discharges of neurons rather than by uncoordinated increases in their firing rates (reviewed in Bruno, 2011). For example, the degree of millisecond-timescale synchrony among TC neurons and consequent L4 discharges varies

depending on features of whisker stimuli (Bruno and Sakmann, 2006; Temereanca et al., 2008; Wang et al., 2010). Experience-induced reduction in TC axonal arborization in and of itself would reduce the common input shared by cortical neurons, which in the simplest case would decrease correlated discharges among L4 neurons during sensory stimulation.

Our data show, however, that reduced TC innervation does not guarantee reduced L4 synchrony, indicating that additional elements of the thalamocortical circuit are plastic. The loss of afferent input might additionally trigger homeostatic rescaling of the strength of synapses—afferent and/or intracortical—onto an excitatory L4 neuron to maintain its normal firing rate. Consistent with this possibility, we observed that trimming enhances the strengths of common inputs shared by L4 neurons. Synaptic rescaling of intracortical connections within layer 4 is thought to switch off during development but has not yet been studied for thalamocortical connections (Turrigiano, 2011). Reduced TC innervation may directly or indirectly lead to potentiation of unpruned TC synapses.

An additional possibility, not mutually exclusive, is that inhibitory synapses are homeostatically weakened or removed, producing the strengthening of shared excitatory inputs we observed. Consistent with this, sensory experience in adults alters the density of inhibitory corticocortical connections, which is increased by overstimulation as seen ultrastructurally (Knott et al., 2002) and decreased after deprivation as observed via glutamic acid decarboxylase staining or GABA receptor radiolabeling (Akhtar and Land, 1991; Fuchs and Salazar, 1998). Future studies, such as minimal stimulation of TC axons and paired recordings from connected cortical cells in vitro, are needed to assess the relative contributions of thalamocortical strengthening, inhibitory synapse weakening or pruning, and their induction times to L4 synchrony. Changes in L4 synchrony may partially explain why trimming suppresses L2/3 responses during adolescence but not adulthood (Glazewski and Fox, 1996).

Our results clearly show that innocuous, nondestructive sensory experience during adulthood induces large-scale changes in thalamocortical axons. This contradicts the idea that adult plasticity has a purely cortical locus and raises the possibility that the structure of other subcortical regions might remain in flux throughout life. Subcortical connections, such as primary afferents traversing the spinal cord or brainstem fibers ascending to thalamus, may be more plastic than currently thought. While largely stable in their branching patterns and size, axons from superficial and deep cortical layers as well as nonprimary thalamic nuclei continuously elongate and retract short branches in wild-type animals (De Paola et al., 2006). Our study indicates that axons from primary thalamic nuclei exhibit similar ongoing structural dynamics. Changes in sensory experience, whether by experimental manipulation (e.g., trimming) or in the natural environment, probably stabilize and destabilize axonal bouton/branch turnover, slowly sculpting out new axonal morphology and patterns of connectivity. Rapid spine turnover is known to exist on dendritic trees with otherwise stable morphology in motor, somatosensory, and visual cortices (Grutzendler et al., 2002; Trachtenberg et al., 2002; Xu et al., 2009). Our study indicates that experience-induced plasticity involves not only synaptic strengthening/weakening and fine-scale formation/ pruning of synapses but also gross axonal remodeling.

We conclude that thalamocortical input to cortex remains plastic in adulthood, raising the possibility that the axons of other subcortical structures might also remain in flux throughout life.

EXPERIMENTAL PROCEDURES

All procedures were approved by the Columbia University Institutional Animal Care and Use Committee. Twenty-eight adult (weight 200–500 g, mean 290 g) Wistar rats (Hilltop Laboratories) were used for anatomy experiments. All whiskers except two (D2 and D3) on the right side of the face were trimmed to a length of <1 mm every second day, without anesthesia, for 13–27 days prior to cell filling. All whiskers on the left side of the face were trimmed. Two whiskers were spared, as opposed to trimming off all whiskers bilaterally, to ensure that animals continued to explore the environment via the whisker system. Deprived rats continued to whisk over large arcs and actively palpate objects and surfaces with their spared whiskers. Deprived rats were housed in the same cages as control littermates, which were handled similarly. Control rats were sham trimmed by gently brushing the whiskers with scissors. Cages were enriched with cardboard boxes or tubes to encourage whisker use.

Cell Filling

Rats were initially anesthetized with isoflurane and then transferred to urethane (1.6 g/kg intraperitoneally; 10% supplements as needed). Body temperature was maintained at 37°C by a heating blanket. The parietal and occipital bones were exposed, and a metal post for positioning the head was attached to the skull using dental acrylic. The skull overlying the ventral posterior medial thalamic nucleus of the left hemisphere was thinned with a dental drill until transparent, and a craniotomy was opened (~2 mm^2, centered 3.0 mm posterior to bregma and 3.5 mm lateral of the midline).

Thalamus was mapped extracellularly by conventional means. Glass pipettes with tips of ~5 μm inside diameter (ID) were filled with artificial cerebrospinal fluid (aCSF; 135 mM NaCl, 5.4 mM KCl, 1.8 mM $CaCl_2$, 1.0 mM $MgCl_2$, and 5.0 mM HEPES [pH 7.2]) and inserted vertically to a microdrive depth of 4,700–5,700 μm. Signals were amplified, band-pass filtered at 0.3–9 kHz, and played over an audio monitor. Whiskers were deflected manually using hand-held probes to determine the principal whisker corresponding to any given location.

Cells were filled by whole-cell recording. Patch pipettes were pulled from 2 mm unfilamented borosilicate glass. Tip ID was ~0.5 μm. Pipettes were tip filled with 135 mM K-gluconate, 10 mM HEPES, 10 mM phosphocreatine-Na_2, 4 mM KCl, 4 mM ATP-Mg, 0.3 mM GTP, and 1% biocytin (pH 7.2). Cells were searched for in voltage-clamp mode using pulses. Whole-cell recordings were made in bridge mode for 15–40 min. We subsequently allowed 12–19 hr to elapse to permit adequate tracer diffusion. To ensure accurate axonal reconstruction, we usually filled only one neuron per rat. Occasionally, additional neurons were filled but, in these cases, they would be targeted 2–3 barreloids away from previous penetrations.

Histology

The rat was deeply anesthetized and perfused transcardially with cold 0.1 M sodium phosphate buffer followed by 4% paraformaldehyde (in 0.1 M buffer). Barrel cortex was cut tangentially in 50 μm sections on a freezing microtome, and thalamus was cut coronally in 100 μm sections. Sections were stained for cytochrome oxidase (CO) and subsequently biocytin. Twenty-five cells out of a total of 37 filled ones were recovered.

3D Semiautomated Reconstruction of Neuron Morphology

Approximately 40 sections, spanning from the pia to the white matter, were reconstructed per neuron. Axonal branches were detected and traced using a previously described automated method (Oberlaender et al., 2007). In each section, stacks of ~1.5 mm × 1.5 mm

× 0.05 mm were imaged using optimized mosaic optical-sectioning microscopy (Oberlaender et al., 2009) and an oil-immersion objective (Olympus 100× UPLAN S APO, NA 1.4), yielding a voxel size of 0.184 µm × 0.184 µm × 0.5 µm. Manual postprocessing of individual sections (Dercksen et al., 2012), as well as automated alignment of reconstructed branches across sections (Dercksen et al., 2009), was performed using a custom-designed three-dimensional (3D) editing environment based on ZIBamira visualization software v2010.06 (Zuse Institute Berlin). Pia and barrel outlines were manually traced in each section at low resolution (Olympus 4× UPLAN S APO, NA 0.16) and added to the tracings in Neurolucida software (MicroBrightfield).

Morphological Analysis

Reconstructions were placed into a standardized coordinate system. The origin was defined as the center of the L4 barrel that contained the majority of the neuron's axon ("the principal barrel"). The z axis was set to point dorsally, parallel to the vertical axis of the principal barrel. The x axis was defined as the line joining the centers of the principal barrel and the first rostrally neighboring barrel within the same row. Measurements were performed in ZIBamira and double checked in NeuroExplorer v9.03 (MicroBrightfield).

Axon length per individual column was determined by extrapolating the respective L4 barrel contours, rather than idealized barrels, along the vertical axis toward the pia and white matter. Supragranular, granular, and infragranular projections (i.e., above, within, and below the principal barrel) were measured for each column individually because barrel height varied between columns.

Average interbouton distances were obtained from high-resolution image stacks (100× objective, 0.2 µm optical sections). Horizontally projecting axonal segments were randomly selected for analysis because varicosities are difficult to unambiguously identify when an axon travels along the optical axis (vertically). Interbouton distances were determined by manually marking the 3D location of each bouton along the reconstructed axons. Custom-written ZIBamira routines were used to measure distance along the axons between these markers. Measurements were performed for 1,835 boutons from axonal segments in ten different rats (six control and four deprived). IgorPro (Wave-Metrics) was used for statistical analysis of morphological data.

All reconstructions, analyses, and bouton counting were performed double blind (i.e., control and deprived groups were only known after reconstructions and analyses were finalized).

Physiology

An additional 11 adult rats were used for physiology experiments. Prior to surgery, whiskers were trimmed (n = 6) or sham trimmed (n = 5) for 8–25 days. Rats were initially anesthetized with isoflurane. A single craniotomy was made over a thin region of skull overlying the left barrel cortex (0.2 × 1.0 mm; centered 2.5 mm posterior to bregma and 5.5 mm lateral of the midline). Screws were inserted in the right frontal and occipital bones for electrocorticogram recording. Head posts were attached and body temperature maintained as above. The right jugular was cannulated for intravenous drug infusion, the left femoral artery was cannulated for blood pressure monitoring, and a tracheotomy performed. The animal was then transferred to a respirator and continuously infused with intravenous fentanyl (~10 µg/kg/hr). To prevent spontaneous whisker movement, we induced neuromuscular blockade with pancuronium bromide (1.6 mg/kg/hr). A computer monitored electrocorticogram, mean arterial pressure, arterial pulse rate, and tracheal airway pressure.

Experiments were terminated if any of these indicators could not be maintained within normal physiological range.

Extracellular recordings were made from pairs of neurons located in the same barrel using two pipettes. Initially, the barrel field was mapped as above. A mapping pipette normal to the pial surface was used to locate the barrel corresponding to the principal whisker (PW). The correct spatial location was triangulated for another pipette 45° from normal that would place its tip 50 µm away from the first pipette. Proper placement was confirmed by mapping. Once barrel locations relative to the vasculature were determined, recording pipettes (ID < 1 µm; filled with aCSF containing 2% biocytin) were advanced slowly into the barrel cortex to obtain loose-seal cell-attached recordings from pairs. At the end of the experiment, recording sites were confirmed by juxtasomal filling or ejection of biocytin into the extracellular space.

A multidirectional piezoelectric stimulator was used to move the PW in the eight cardinal directions randomized across trials. For both control and deprived animals, a stimulator was placed ~2 mm from the base of the hair and deflected 14° (500 µm amplitude) using high-velocity (measured average velocity ~1,400°/s, measured peak velocity ~3,200°/s) ramp-and-hold movements. The whisker was held for a 200 ms period between stimulus onset and offset.

Physiological data was analyzed using custom-written routines in MATLAB. Coherence analysis was performed using the Chronux toolbox (http://chronux.org). The strength of near-synchronous correlations was assessed using a simple common measure that normalized for the firing rates of the two neurons:

$$strength = \frac{N_c}{\sqrt{(N_1^2 + N_2^2)/2}}$$

where N_c is the sum of shift-corrected events over −5 to +5 ms and N_1 and N_2 are the numbers of cell 1 and cell 2 spikes used to compute the raw correlogram (Bruno and Sakmann, 2006).

Statistical Methods

Control and deprived data were compared nonparametrically using the Wilcoxon rank-sum test, except where otherwise noted. Substituting nonparametric tests with parametric ones did not change the qualitative significance of any of the results.

Supplementary Material

Refer to Web version on PubMed Central for supplementary material.

Acknowledgments

References

Akhtar ND, Land PW. Activity-dependent regulation of glutamic acid decarboxylase in the rat barrel cortex: effects of neonatal versus adult sensory deprivation. J Comp Neurol. 1991; 307:200–213. [PubMed: 1713230]

Antonini A, Stryker MP. Rapid remodeling of axonal arbors in the visual cortex. Science. 1993; 260:1819–1821. [PubMed: 8511592]

Antonini A, Fagiolini M, Stryker MP. Anatomical correlates of functional plasticity in mouse visual cortex. J Neurosci. 1999; 19:4388–4406. [PubMed: 10341241]

Arnold PB, Li CX, Waters RS. Thalamocortical arbors extend beyond single cortical barrels: an in vivo intracellular tracing study in rat. Exp Brain Res. 2001; 136:152–168. [PubMed: 11206278]

Bruno RM. Synchrony in sensation. Curr Opin Neurobiol. 2011; 21:701–708. [PubMed: 21723114]

Bruno RM, Sakmann B. Cortex is driven by weak but synchronously active thalamocortical synapses. Science. 2006; 312:1622–1627. [PubMed: 16778049]

Bruno RM, Hahn TT, Wallace DJ, de Kock CP, Sakmann B. Sensory experience alters specific branches of individual corticocortical axons during development. J Neurosci. 2009; 29:3172–3181. [PubMed: 19279254]

De Paola V, Holtmaat A, Knott G, Song S, Wilbrecht L, Caroni P, Svoboda K. Cell type-specific structural plasticity of axonal branches and boutons in the adult neocortex. Neuron. 2006; 49:861–875. [PubMed: 16543134]

Dercksen, VJ.; Oberlaender, M.; Sakmann, B.; Hege, H-C. Interactive visualization—a key prerequisite for reconstruction of anatomically realistic neural networks. In: Linsen, L.; Hagen, H.; Hamann, B.; Hege, H-C., editors. Visualization in Medical and Life Sciences II. Berlin: Spinger-Verlag; 2012. p. 27-44.

Dercksen, VJ.; Weber, B.; Günther, D.; Oberlaender, M.; Prohaska, S.; Hege, H-C. Automatic alignment of stacks of filament data. Proceedings of the IEEE International Symposium on Biomedical Imaging; 2009. p. 971-974.

Eggermont JJ, Smith GM. Neural connectivity only accounts for a small part of neural correlation in auditory cortex. Exp Brain Res. 1996; 110:379–391. [PubMed: 8871097]

Feldman DE, Brecht M. Map plasticity in somatosensory cortex. Science. 2005; 310:810–815. [PubMed: 16272113]

Feldman DE, Nicoll RA, Malenka RC. Synaptic plasticity at thalamocortical synapses in developing rat somatosensory cortex: LTP, LTD, and silent synapses. J Neurobiol. 1999; 41:92–101. [PubMed: 10504196]

Ferster D, LeVay S. The axonal arborizations of lateral geniculate neurons in the striate cortex of the cat. J Comp Neurol. 1978; 182:923–944. [PubMed: 103938]

Fox K. A critical period for experience-dependent synaptic plasticity in rat barrel cortex. J Neurosci. 1992; 12:1826–1838. [PubMed: 1578273]

Fox K. Anatomical pathways and molecular mechanisms for plasticity in the barrel cortex. Neuroscience. 2002; 111:799–814. [PubMed: 12031405]

Fuchs JL, Salazar E. Effects of whisker trimming on GABA(A) receptor binding in the barrel cortex of developing and adult rats. J Comp Neurol. 1998; 395:209–216. [PubMed: 9603373]

Glazewski S, Fox K. Time course of experience-dependent synaptic potentiation and depression in barrel cortex of adolescent rats. J Neurophysiol. 1996; 75:1714–1729. [PubMed: 8727408]

Grutzendler J, Kasthuri N, Gan WB. Long-term dendritic spine stability in the adult cortex. Nature. 2002; 420:812–816. [PubMed: 12490949]

Jacob V, Petreanu L, Wright N, Svoboda K, Fox K. Regular spiking and intrinsic bursting pyramidal cells show orthogonal forms of experience-dependent plasticity in layer V of barrel cortex. Neuron. 2012; 73:391–404. [PubMed: 22284191]

Jarvis MR, Mitra PP. Sampling properties of the spectrum and coherency of sequences of action potentials. Neural Comput. 2001; 13:717–749. [PubMed: 11255566]

Karmarkar UR, Dan Y. Experience-dependent plasticity in adult visual cortex. Neuron. 2006; 52:577–585. [PubMed: 17114043]

Khibnik LA, Cho KK, Bear MF. Relative contribution of feed-forward excitatory connections to expression of ocular dominance plasticity in layer 4 of visual cortex. Neuron. 2010; 66:493–500. [PubMed: 20510854]

Knott GW, Quairiaux C, Genoud C, Welker E. Formation of dendritic spines with GABAergic synapses induced by whisker stimulation in adult mice. Neuron. 2002; 34:265–273. [PubMed: 11970868]

Oberlaender M, Bruno RM, Sakmann B, Broser PJ. Transmitted light brightfield mosaic microscopy for three-dimensional tracing of single neuron morphology. J Biomed Opt. 2007; 12:064029. [PubMed: 18163845]

Oberlaender M, Broser PJ, Sakmann B, Hippler S. Shack-Hartmann wave front measurements in cortical tissue for deconvolution of large three-dimensional mosaic transmitted light brightfield micrographs. J Microsc. 2009; 233:275–289. [PubMed: 19220694]

Oberlaender M, Boudewijns ZS, Kleele T, Mansvelder HD, Sakmann B, de Kock CP. Three-dimensional axon morphologies of individual layer 5 neurons indicate cell type-specific intracortical pathways for whisker motion and touch. Proc Natl Acad Sci USA. 2011; 108:4188–4193. [PubMed: 21368112]

Smith PH, Uhlrich DJ, Manning KA, Banks MI. Thalamocortical projections to rat auditory cortex from the ventral and dorsal divisions of the medial geniculate nucleus. J Comp Neurol. 2012; 520:34–51. [PubMed: 21618239]

Temereanca S, Brown EN, Simons DJ. Rapid changes in thalamic firing synchrony during repetitive whisker stimulation. J Neurosci. 2008; 28:11153–11164. [PubMed: 18971458]

Trachtenberg JT, Trepel C, Stryker MP. Rapid extragranular plasticity in the absence of thalamocortical plasticity in the developing primary visual cortex. Science. 2000; 287:2029–2032. [PubMed: 10720332]

Trachtenberg JT, Chen BE, Knott GW, Feng G, Sanes JR, Welker E, Svoboda K. Long-term in vivo imaging of experience-dependent synaptic plasticity in adult cortex. Nature. 2002; 420:788–794. [PubMed: 12490942]

Turrigiano G. Too many cooks? Intrinsic and synaptic homeostatic mechanisms in cortical circuit refinement. Annu Rev Neurosci. 2011; 34:89–103. [PubMed: 21438687]

Wallace H, Fox K. The effect of vibrissa deprivation pattern on the form of plasticity induced in rat barrel cortex. Somatosens Mot Res. 1999; 16:122–138. [PubMed: 10449061]

Wang Q, Webber RM, Stanley GB. Thalamic synchrony and the adaptive gating of information flow to cortex. Nat Neurosci. 2010; 13:1534–1541. [PubMed: 21102447]

Wimmer VC, Broser PJ, Kuner T, Bruno RM. Experience-induced plasticity of thalamocortical axons in both juveniles and adults. J Comp Neurol. 2010; 518:4629–4648. [PubMed: 20886626]

Xu T, Yu X, Perlik AJ, Tobin WF, Zweig JA, Tennant K, Jones T, Zuo Y. Rapid formation and selective stabilization of synapses for enduring motor memories. Nature. 2009; 462:915–919. [PubMed: 19946267]
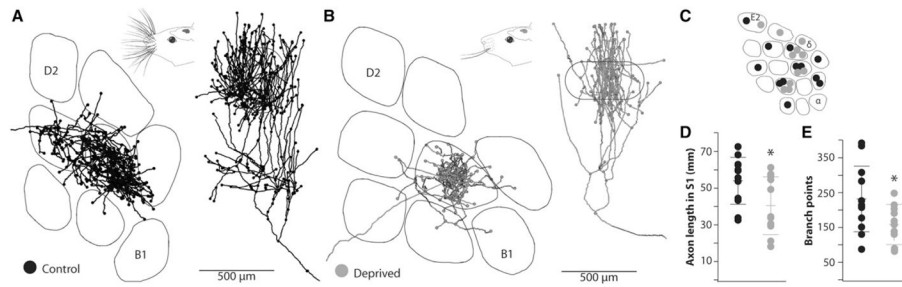
Figure 1. Whisker Trimming during Adulthood Substantially Reduces the Length of Thalamocortical Axons

(A and B) Reconstructions of thalamocortical axons in control (A) and deprived (B) animals, respectively. Axons in deprived animals correspond to trimmed whiskers. Left, tangential view; right, radial view; lines, barrel borders; dots, branch points and end points. Insets: adult rats were sham trimmed (A) or had all whiskers but two trimmed off (B). (C) Columns targeted by control (black) and deprived (gray) axons. The position of symbols within any given column is arbitrary. (D) Distributions of total axon lengths within cortex. Lines represent means ± SD. (E) Distributions of branch points within cortex. Lines represent means ± SD.
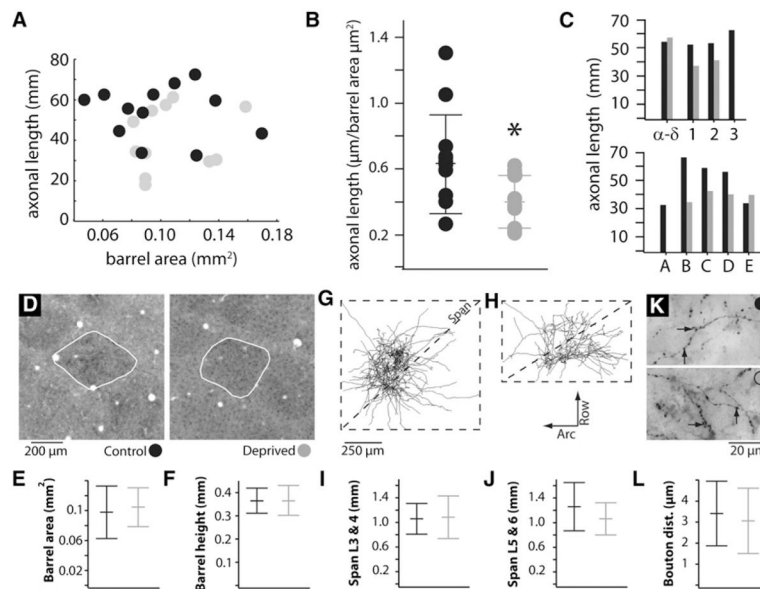
Figure 2. Other Morphological Features Appear Unrelated to Differences in Axonal Length
(A) There is no significant relationship of the length of thalamocortical axon to the size of the barrel innervated, regardless of whether control (black) and deprived (gray) groups are analyzed separately or pooled (all p values > 0.5). (B) Control and deprived groups differ even after normalizing the lengths of axons to the areas of their respective barrels (p = 0.03). (C) Axonal length is relatively uniform across arcs (top) and rows (bottom), with deprivation having a relatively consistent effect at all locations. (D) Tangential section through the barrel field of a control (left) and a deprived (right) rat. (E and F) Trimming did not alter mean area occupied by barrels in tangential plane (E) or thickness in the radial dimension (F). Lines represent means ± SD. (G and H) Field span was calculated along a diagonal separately for L3/4 (G) and L5/6 (H) branches. (I and J) Distributions of field spans for L3/4 (I) and L5/6 (J) branches. (K) Axonal varicosities in a control (top) and a deprived (bottom) rat. (L) Distributions of inter-bouton distances along a randomly selected subset of axonal branches. Lines represent means ± SD for (B), (I), (J), and (L).
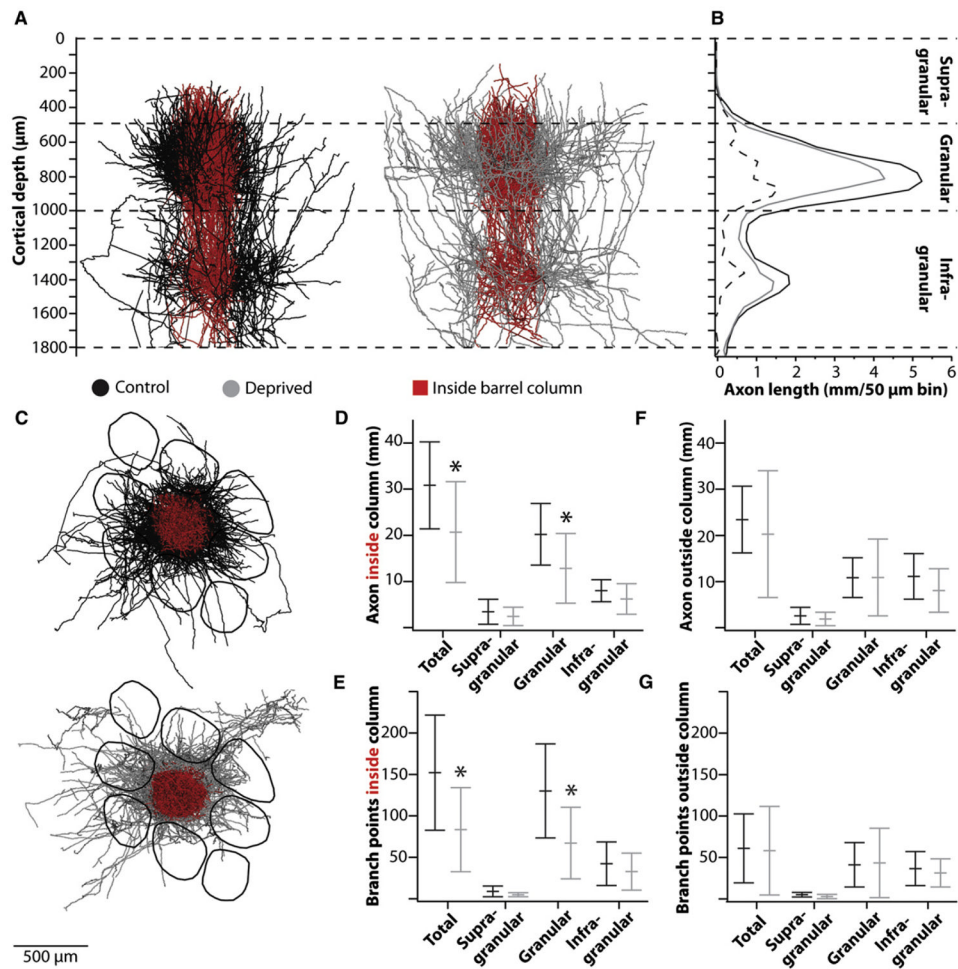
Figure 3. Axonal Remodeling Is Limited to Specific Branches

(A) Overlays of all axons for control (left) and deprived (right) animals. Red, axon inside the column as defined by borders of the targeted barrel. (B) Length of axon by depth from pia for each group. Dashed line, difference between groups. (C) Tangential views of overlaid axons. An example partial barrel field is overlaid purely to further illustrate scale. As shown in Figure 1C, the axons most densely innervated a variety of different barrels rather than the same barrel. (D and F) Axon lengths, total and by layer, inside (D) and outside (F) the targeted columns. (E and G) Same as (D) and (F) for branch points. Lines represent means ± SD.
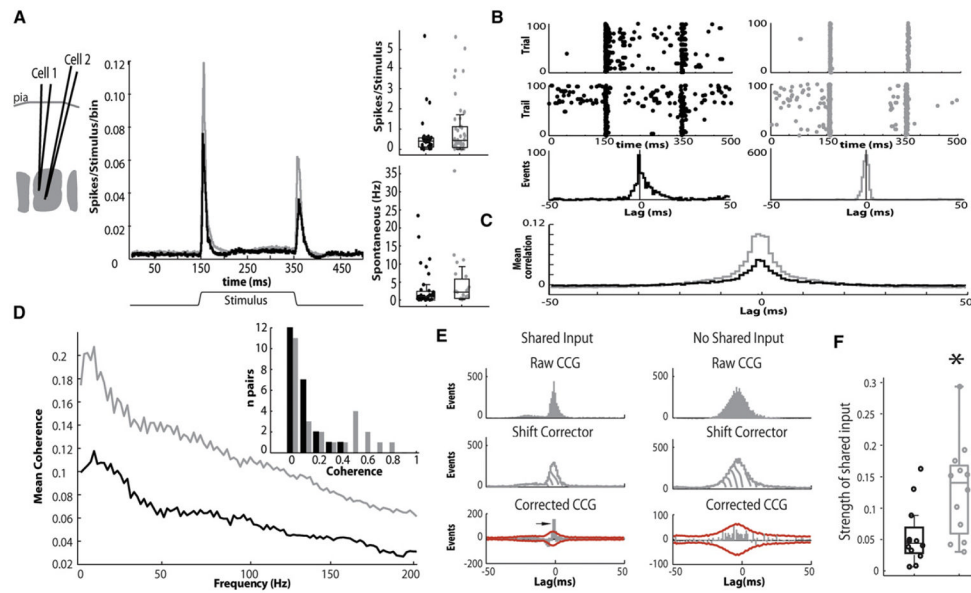
Figure 4. Experience Alters the Synchrony, but Not Magnitude, of Sensory-Evoked Activity among Cortical Layer 4 Neurons
(A) Dual cell-attached recordings were made from the same barrel in control and deprived animals (left), and peristimulus time histograms for each population were plotted (middle). Evoked and spontaneous firing rates are plotted for individual cells (right). Box plots show medians and interquartile ranges. (B) Example rasters and cross-correlograms for a control pair (left) and deprived pair (right). (C) Mean firing rate normalized cross-correlograms for each group. The cross-correlogram of each pair was normalized by the geometric mean of the two cells' firing rates. (D) Coherence functions averaged over all pairs. Inset: individual coherence values for each pair (mean over 4–20 Hz). (E) Examples of pairs with (left) and without (right) signs of shared synaptic inputs. Both pairs were recorded in trimmed rats. The raw cross-correlogram (CCG) measures total correlated activity of a pair of neurons (top). The shift corrector (middle), the recalculation of the correlogram after shifting one of the spike trains by a trial, measures stimulus-induced correlation. The corrected cross-correlogram (bottom) is their difference. A peak exceeding 3.3 standard deviations (α = 0.001) of the shift corrector (red lines) is taken as evidence of significant shared synaptic input (arrow). (F) Distributions of the strength of significant shared synaptic inputs for individual pairs (circles). Box plots show medians and interquartile ranges.